

# MULTIMODAL WIRELESS NETWORKS: DISTRIBUTED SURVEILLANCE WITH MULTIPLE NODES

*Zoltan Safar, John Aa. Sørensen, Jianjun Chen, and Kåre J. Kristoffersen*  
Department of Innovation, IT University of Copenhagen, Copenhagen, Denmark

## ABSTRACT

Multimodal wireless networks are wireless networks that offer multiple functionalities realized on the same infrastructure. In this paper, we consider a multimodal network that has two modes of operation: the communication mode, when the network is used as a traditional wireless communication network, and the surveillance mode, when the network is used as a distributed sensor network that can detect illegal intrusion by detecting changes in the propagation environment caused by the intruder. We address the problem of distributed surveillance in a network consisting of multiple nodes: we develop a multi-sensor model for the received signal parameters of interest and derive a detector capable of detecting changes in these parameters. The experimental results demonstrate that combining the information from different nodes with the appropriate fusion function results in considerably improved detection performance compared to that of single-node detectors.

## 1. INTRODUCTION

In the past few years, wireless networks have become widespread, and they are gaining popularity day by day. Wireless devices, such as wireless-enabled laptops and palm pilots, have become an integral part of our daily lives. In the near future, wireless networks will be ubiquitous, offering high-speed communication capabilities almost everywhere. Thus, the question arises naturally: is it possible to use the wireless network infrastructure to implement other functionalities in addition to communication?

The answer is given by recognizing that a wireless network can be considered as a sensor network, where the network nodes also function as sensors. They sense changes in the propagation environment due to moving objects or humans, so a possible additional functionality could be indoor surveillance of corporate buildings and private houses. So far, the problems of wireless communication and "physical" intrusion detection (i.e. detecting a person or persons entering private/corporate premises illegally) have been considered as two separate issues, and two different infrastructures have been deployed: one for communication and one for surveillance/security. However, if the communication infrastructure could also be used for security purposes, the deployment of the additional infrastructure could be avoided or reduced, resulting in a considerably more cost-effective solution.

Previous experiments investigating the impact of moving objects/humans on the propagation environment [1], [2]

have shown that significant variations can be observed in the received signal strength and the rms delay spread. However, those measurements were carried out using specialized equipment, and not low-cost, off-the-shelf devices, such as a WLAN card, and the authors did not propose any signal processing architectures or algorithms for intrusion detection.

In [3], we proposed the idea of multimodal wireless networks: networks that can offer multiple functionalities realized on the same infrastructure. The multimodal wireless networks have two modes of operation: the communication mode, when the network is used as a traditional WLAN or WPAN, and the surveillance mode, when the communication network is used as a distributed sensor network that can detect illegal intrusion. We also described a single-receiver (or single-sensor) model for the received signal parameter of interest (e.g. time of arrival or signal strength) and derived a detector for detecting change in that parameter.

In this paper, we consider the problem of distributed surveillance with multiple wireless network nodes. We develop a multi-sensor model for the received signal parameters, taking into account their quantized nature and inaccuracy due to signal measurement values that are not calibrated or not standardized. Moreover, we derive a parameter change detector based on the generalized likelihood ratio test (GLRT) for a multiple transmitter/multiple receiver scenario. The novelty of this work compared to [3] lies in the generalization of the detector for the multi-sensor case, the derivation of methods for the joint estimation of multiple parameters for each node, and the solution to the information fusion problem, which comes naturally from the multi-sensor GLRT formulation.

The architecture of the surveillance system is shown in Figure 1. In communication mode, the wireless transceiver nodes (e.g. access points, or nodes in an ad-hoc network) implement the functionality of a traditional wireless network. In surveillance mode, the nodes transmit, for example, one by one in a round robin fashion, and the rest of the nodes receive the transmitted signal. First, the received signal at each node is processed by a preprocessor to extract the relevant characteristics of the propagation environment, called features, which may include time of arrival, angle of arrival, the strength of the received signal, channel impulse response, or a combination of these. The obtained set of such features is then combined by an information fusion function, which produces a single output that is used to decide whether an intruder is present in the system or not.

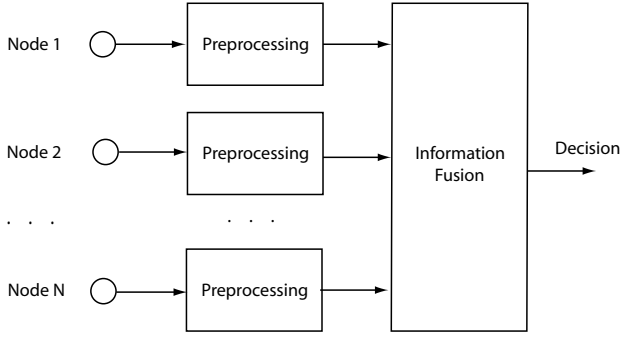


Fig. 1. The architecture of the surveillance system

## 2. SIGNAL MODEL AND PROBLEM SETUP

Consider a wireless network consisting of  $N$  nodes. During scanning period  $m$  ( $1 \leq m \leq N$ ), only node  $m$  transmits  $T$  times, and the rest of the nodes receive the transmitted signal. The model of the received signal parameter of interest at node  $n$  ( $1 \leq n \leq N$ ,  $n \neq m$ ) at discrete time  $t$  ( $1 \leq t \leq T$ ) of scanning period  $m$  can be observed in Figure 2. The true value of the received signal parameter,  $l_{m,n}^0$ , is shifted by an unknown bias,  $B_{m,n}$ , resulting in the biased parameter,  $l_{m,n}$ , which is assumed to take on values between  $l_{MIN}$  and  $l_{MAX}$ . The bias represents measurement inaccuracy due to transmitted and received signal features that are not calibrated and/or not standardized, such as the 802.11 transmit power and RSSI value calculation. Note that due to the bias, in general,  $l_{m,n} \neq l_{n,m}$ , even if the channel is reciprocal. The true signal parameter is further disturbed with zero-mean, white Gaussian noise  $z_{m,n}(t)$  with variance  $\sigma_n^2$  at discrete time  $t$ . The observed values are usually only available in quantized form (for example, 802.11 RSSI values), so the observations are  $\{y_{m,n}(t)\}$ , the quantizer indices corresponding to the noisy and biased signal parameter values  $\{x_{m,n}(t)\}$ . The quantizer is assumed to have  $N_q = 2^b$  levels, where  $b$  is the number of bits representing the signal parameter. The decision regions are denoted by  $a(0) < a(1) < \dots < a(N_q)$ , with  $a(0) = -\infty$  and  $a(N_q) = +\infty$ , and the quantizer maps the input value  $x$  to the quantizer index  $y \in \{0, 1, \dots, N_q - 1\}$  if  $a(y) < x \leq a(y+1)$ .

Our objective is to detect changes  $\Delta l_{m,n}$  with respect to the true signal parameters  $l_{m,n}^0$  given the observation vector  $\mathbf{y} = \{y_{m,n}(t)\}$ . The two detection hypotheses can be formulated as follows:  $\mathcal{H}_0$ : no change detected (no intruder present), and  $\mathcal{H}_1$ : change detected (intruder present). Since the detection of change is not affected by the bias  $B_{m,n}$ , the true values of the signal parameters are not needed for our purposes, and we can equivalently base our decision on the biased parameters  $l_{m,n}$ .

The detection procedure will consist of the following two phases: the training phase and the detection phase. During the training phase, the steady state of the propagation environment is estimated. The signal (and noise) parameters  $l_{m,n}$  and  $\sigma_n$  are not known, so they must be estimated when it is ensured that  $\mathcal{H}_0$  is true (i.e. no intruder). The quantities  $l_{m,n}$  and  $\sigma_n$  are obtained by developing an approximate

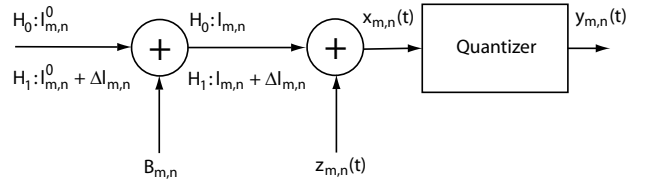


Fig. 2. The received signal model

and an iterative maximum likelihood (ML) estimator using a larger number ( $T = 1000$ ) of training samples. This can be done during a couple of seconds when the surveillance system is armed. Note that this step is necessary since the propagation environment may change significantly during an inactive period of the surveillance system. For example, workers at a company may move furniture or leave doors open or closed during daytime.

The second phase is the detection phase, when the surveillance system detects the changes  $\Delta l_{m,n}$  in the parameters  $l_{m,n}$  based on a small number ( $T = 50$ ) of observations. Since the probability of detection must be maximized for a given probability of false alarm, the detection problem will be formulated as a GLRT. Again, the values of  $\Delta l_{m,n}$  for the  $\mathcal{H}_1$  case are estimated by an approximate and an iterative ML estimator.

## 3. TRAINING PHASE

Given an observation vector  $\mathbf{y}$  (now  $T$  represents the training data record length), we would like to estimate the values  $l_{m,n}$  and  $\sigma_n$ . The log-likelihood function of the parameters  $\mathbf{l} = \{l_{m,n}\}$  and  $\boldsymbol{\sigma} = \{\sigma_n\}$  is given by

$$\ln P(\mathbf{y} = \mathbf{i}; \mathbf{l}, \boldsymbol{\sigma}) = \sum_{n=1}^N \sum_{m=1}^N \sum_{t=1}^T \ln G(l_{m,n}, \sigma_n, a_{m,n}^-(t), a_{m,n}^+(t)), \quad (1)$$

where  $\mathbf{i} = \{i_{m,n}(t)\}$  is an observed realization of the random vector  $\mathbf{y}$ ,  $a_{m,n}^-(t) = a(i_{m,n}(t))$ ,  $a_{m,n}^+(t) = a(i_{m,n}(t) + 1)$ , and the function  $G(\cdot)$  is defined as

$$G(l, \sigma, \alpha, \beta) = \frac{1}{\sqrt{2\pi}\sigma} \int_{\alpha}^{\beta} e^{-\frac{(\nu-l)^2}{2\sigma^2}} d\nu = Q\left(\frac{\alpha-l}{\sigma}\right) - Q\left(\frac{\beta-l}{\sigma}\right).$$

The ML estimate of the parameters for node  $n$  can be obtained by finding the values  $l_{m,n}$ ,  $1 \leq m \leq N$ ,  $m \neq n$ , and  $\sigma_n$  such that  $\frac{\partial}{\partial l_{m,n}} \ln P(\mathbf{y} = \mathbf{i}; \mathbf{l}, \boldsymbol{\sigma}) = 0$  and  $\frac{\partial}{\partial \sigma_n} \ln P(\mathbf{y} = \mathbf{i}; \mathbf{l}, \boldsymbol{\sigma}) = 0$ , yielding the conditions

$$f_1(l_{m,n}, \sigma_n) = \sum_{t=1}^T \frac{X(l_{m,n}, \sigma_n, a_{m,n}^-(t)) - X(l_{m,n}, \sigma_n, a_{m,n}^+(t))}{G(l_{m,n}, \sigma_n, a_{m,n}^-(t), a_{m,n}^+(t))} = 0$$

$$f_2(l_n, \sigma_n) = \sum_{m=1}^N \sum_{t=1}^T \psi(l_{m,n}, \sigma_n, a_{m,n}^-(t), a_{m,n}^+(t)) = 0,$$

where  $X(l, \sigma, \alpha) = \exp(-(\alpha - l)^2 / 2\sigma^2)$ , the vector  $\mathbf{l}_n$  is given by  $\mathbf{l}_n = [l_{1,n}, l_{2,n}, \dots, l_{n-1,n}, l_{n+1,n}, \dots, l_{N,n}]^T$ , and

$$\psi(l, \sigma, \alpha, \beta) = \frac{(\alpha-l)X(l, \sigma, \alpha) - (\beta-l)X(l, \sigma, \beta)}{G(l, \sigma, \alpha, \beta)}.$$

The solution cannot be obtained in closed form, so we derive an approximate ML estimator and an iterative ML estimator.

The approximate ML estimator is obtained by approximating the integral of  $G(\cdot)$  as  $\int_{\alpha}^{\beta} f(x)dx \approx f(\frac{\alpha+\beta}{2})(\beta - \alpha)$ . As a result, the approximate log-likelihood function becomes

$$\ln P(\mathbf{y} = \mathbf{i}; \mathbf{l}, \sigma) \approx \sum_{n=1}^N \sum_{\substack{m=1 \\ m \neq n}}^N \sum_{t=1}^T -\ln(\sqrt{2\pi}\sigma_n) - \frac{1}{2\sigma_n^2} \left( \frac{a_{m,n}^-(t) + a_{m,n}^+(t)}{2} - l_{m,n} \right)^2 + \ln(a_{m,n}^+(t) - a_{m,n}^-(t)). \quad (2)$$

By taking its partial derivative with respect to  $l_{m,n}$ , setting it equal to zero and solving for  $l_{m,n}$  yields the estimator

$$\hat{l}_{m,n} = \frac{1}{T} \sum_{t=1}^T \frac{a_{m,n}^-(t) + a_{m,n}^+(t)}{2}, \quad (3)$$

which is the sample mean of the quantized observations for uniform quantizers. Similar, taking the partial derivative with respect to  $\sigma_n^2$ , setting it to zero, solving for  $\sigma_n^2$  and using  $\hat{l}_{m,n}$  for the value of  $l_{m,n}$  gives the estimator

$$\hat{\sigma}_n^2 = \frac{1}{(N-1)T} \sum_{\substack{m=1 \\ m \neq n}}^N \sum_{t=1}^T \left( \frac{a_{m,n}^-(t) + a_{m,n}^+(t)}{2} - \hat{l}_{m,n} \right)^2. \quad (4)$$

When using (3) and (4), the values of  $a(0)$  and  $a(N_q)$  need to be replaced with appropriate finite values.

The iterative ML estimator performs a series of Newton-Raphson iterations using the estimates from the approximate ML estimator as initial values. Let us define the estimated signal parameter vector for node  $n$  at the  $k$ -th iteration as  $\hat{\mathbf{l}}_n^{(k)} = [\hat{l}_{1,n}^{(k)}, \dots, \hat{l}_{n-1,n}^{(k)}, \hat{l}_{n+1,n}^{(k)}, \dots, \hat{l}_{N,n}^{(k)}]^T$ , and let the solution vector for the  $k$ -th iteration be  $\mathbf{s}_n^{(k)} = [\hat{\mathbf{l}}_n^{(k)T}, \hat{\sigma}_n^{(k)}]^T$ . Then, the solution for the next iteration,  $\mathbf{s}_n^{(k+1)}$ , can be obtained by solving

$$\mathbf{D}_n^{(k)}(\mathbf{s}_n^{(k)} - \mathbf{s}_n^{(k+1)}) = \mathbf{f}_n^{(k)}, \quad (5)$$

where

$$\mathbf{D}_n^{(k)} = \begin{bmatrix} \text{diag}(d_{1,n}^{(k)}, \dots, d_{n-1,n}^{(k)}, d_{n+1,n}^{(k)}, \dots, d_{N,n}^{(k)}) & \mathbf{c}_n^{(k)} \\ \mathbf{b}_n^{(k)T} & w_n^{(k)} \end{bmatrix},$$

$$\mathbf{f}_n^{(k)} = [f_1(\hat{l}_{1,n}^{(k)}, \hat{\sigma}_n^{(k)}), \dots, f_1(\hat{l}_{n-1,n}^{(k)}, \hat{\sigma}_n^{(k)}), \dots, f_1(\hat{l}_{n+1,n}^{(k)}, \hat{\sigma}_n^{(k)}), \dots, f_1(\hat{l}_{N,n}^{(k)}, \hat{\sigma}_n^{(k)}), f_2(\hat{\mathbf{l}}_n^{(k)}, \hat{\sigma}_n^{(k)})]^T,$$

and the diagonal entries  $\{d_{m,n}^{(k)}\}$ , the coordinates of the vector  $\mathbf{b}_n^{(k)} = [b_{1,n}^{(k)}, \dots, b_{n-1,n}^{(k)}, b_{n+1,n}^{(k)}, \dots, b_{N,n}^{(k)}]^T$ , the coordinates of the vector  $\mathbf{c}_n^{(k)} = [c_{1,n}^{(k)}, \dots, c_{n-1,n}^{(k)}, c_{n+1,n}^{(k)}, \dots, c_{N,n}^{(k)}]^T$  and  $w_n^{(k)}$  are given by

$$d_{m,n}^{(k)} = \left. \frac{\partial f_1(l_{m,n}, \sigma_n)}{\partial l_{m,n}} \right|_{l_{m,n}=\hat{l}_{m,n}^{(k)}, \sigma_n=\hat{\sigma}_n^{(k)}},$$

$$b_{m,n}^{(k)} = \left. \frac{\partial f_2(\mathbf{l}_n, \sigma_n)}{\partial l_{m,n}} \right|_{\mathbf{l}_n=\hat{\mathbf{l}}_n^{(k)}, \sigma_n=\hat{\sigma}_n^{(k)}},$$

$$c_{m,n}^{(k)} = \left. \frac{\partial f_1(l_{m,n}, \sigma_n)}{\partial \sigma_n} \right|_{l_{m,n}=\hat{l}_{m,n}^{(k)}, \sigma_n=\hat{\sigma}_n^{(k)}},$$

$$w_n^{(k)} = \left. \frac{\partial f_2(\mathbf{l}_n, \sigma_n)}{\partial \sigma_n} \right|_{\mathbf{l}_n=\hat{\mathbf{l}}_n^{(k)}, \sigma_n=\hat{\sigma}_n^{(k)}}.$$

These derivatives can be obtained in closed form after some tedious, but straightforward calculations, and they are omitted here for brevity. The iterations stop if two consecutive solution vectors are closer to each other than a predefined threshold value  $\delta$ .

#### 4. DETECTION PHASE

In the detection phase, the detector observes a quantizer index vector  $\mathbf{y}$  (now the observation period  $T$  is considerably smaller than that for the training phase), and decides whether there is a significant change in the signal parameters  $l_{m,n}$  ( $\mathcal{H}_1$ ) or not ( $\mathcal{H}_0$ ). The detection algorithm is based on the GLRT: decide  $\mathcal{H}_1$  if

$$\frac{P(\mathbf{y} = \mathbf{i}; \mathcal{H}_1)}{P(\mathbf{y} = \mathbf{i}; \mathcal{H}_0)} > \gamma, \quad (6)$$

and  $\gamma$  is the decision threshold. For both hypotheses, the previously estimated  $l_{m,n}$  and  $\sigma_n$  values are used. In addition, for the hypothesis  $\mathcal{H}_1$ , the values of  $\Delta l_{m,n}$  also have to be estimated, while for  $\mathcal{H}_0$ ,  $\Delta l_{m,n} = 0$  is assumed. The values of  $\Delta l_{m,n}$  under  $\mathcal{H}_1$  can be estimated similarly to the method described in Section 3, yielding an approximate and an iterative ML estimator.

By taking the logarithm of (6) and using the estimates of  $\Delta l_{m,n}$  for  $\mathcal{H}_1$ , the GLRT becomes: decide  $\mathcal{H}_1$  if

$$\sum_{n=1}^N g_n > \gamma' = \ln \gamma, \quad (7)$$

and  $g_n$  is given by

$$g_n = \sum_{\substack{m=1 \\ m \neq n}}^N \sum_{t=1}^T \ln G(\hat{\Delta}l_{m,n}, \hat{\sigma}_n, a_{m,n}^-(t) - \hat{l}_{m,n}, a_{m,n}^+(t) - \hat{l}_{m,n}) - \ln G(0, \hat{\sigma}_n, a_{m,n}^-(t) - \hat{l}_{m,n}, a_{m,n}^+(t) - \hat{l}_{m,n}).$$

Comparing the architecture of Figure 1 with (7), the system operation in the detection phase can be summarized as follows. During  $N$  consecutive scanning periods, the preprocessing stage of node  $n$  computes the feature  $g_n$  from its observations, independently of the other nodes (but in coordination with them). Then, these features are sent to the fusion center that performs the summation-in-decision-out information fusion by a simple summation and threshold comparison.

#### 5. EXPERIMENTAL RESULTS

To illustrate the performance of the change detector, we performed some computer simulations and some experiments. The observations were the RSSI values provided by 802.11b ZyAIR B-100 WLAN cards, and the signal parameters  $l_{m,n}$  were the received signal strength values. We used a uniform quantizer matched to the properties of the WLAN card: it had  $N_q = 128$  levels with  $l_{MAX} = 27.5$  dB and  $l_{MIN} = -100.5$  dB, and the decision regions were  $a(i) = l_{MIN} + i\Delta$ ,  $i = 1, 2, \dots, N_q - 1$ , with  $\Delta = (l_{MAX} - l_{MIN})/N_q = 1$ . For the approximate ML estimators, the values  $a(0) = l_{MIN}$  and  $a(N_q) = l_{MAX}$  were used, and for the iterative ML estimators, the convergence threshold was set to  $\delta = 0.05$ .

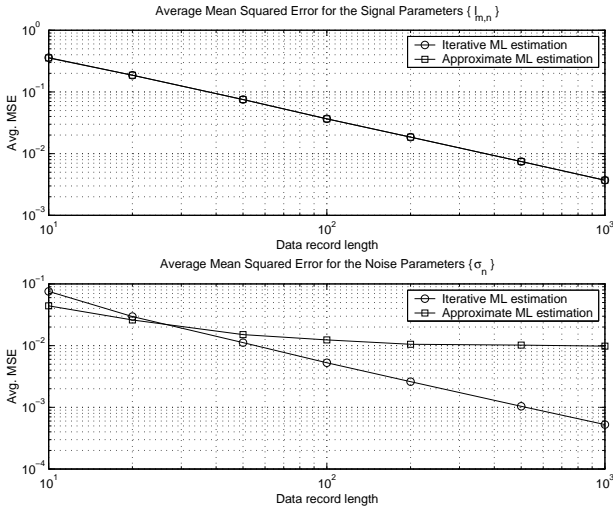


Fig. 3. The performance of the estimator

We investigated the performance of the approximate and the iterative ML estimators via computer simulations. We considered a 3-node system with the parameters:  $l_{1,2} = -32.42$  dB,  $l_{1,3} = -50.11$  dB,  $l_{2,1} = -32.83$  dB,  $l_{2,3} = -41.76$  dB,  $l_{3,1} = -49.88$  dB,  $l_{3,2} = -41.91$  dB,  $\sigma_1^2 = 0.5$ ,  $\sigma_2^2 = 0.4$ ,  $\sigma_3^2 = 0.7$ . The results are shown in Figure 3: the upper part of the figure depicts the average mean squared error (MSE) for the signal parameters  $\{l_{m,n}\}$  as a function of the training data record length, while the lower part depicts the average MSE for the noise parameters  $\{\sigma_n\}$ . From the figures, it can be seen that in case of the signal parameters, both estimators have the same performance. However, in case of the noise parameters, the iterative estimator yields better estimates at longer data record lengths: at  $T = 1000$ , its accuracy is more than one order of magnitude better than that of the approximate ML estimator. If the data record length is very small, the initial values provided by the approximate estimator tend to be further away from the global optimum point, so the iterative estimator will converge to a local optimum point, resulting in worse performance. However, if the data record length is long enough, the iterative method is able to find the global optimum point more often, improving its performance compared to the approximate estimator.

The performance of the detector was evaluated by performing a set of experiments using three laptops with 802.11b WLAN cards as network nodes. One laptop was configured to send beacon frames in every 5 ms, and the two others captured those frames in monitor mode and recorded the received RSSI values. The laptops were separated by several room walls made of plaster, and a wooden door between the transmitter node and the receiver nodes was closed and half-opened ( $45^\circ$ ). The decision hypotheses were:  $\mathcal{H}_0$ : the door is closed, and  $\mathcal{H}_1$ : the door is not closed. For the training phase,  $T = 1000$  samples were used to estimate  $\{l_{m,n}\}$  and  $\{\sigma_n\}$  with the iterative ML estimator when the door was closed. Then, blocks of  $T = 50$  samples were used to detect the signal parameter changes  $\{\Delta l_{m,n}\}$  with the approximate ML estimator. To calculate the average probability

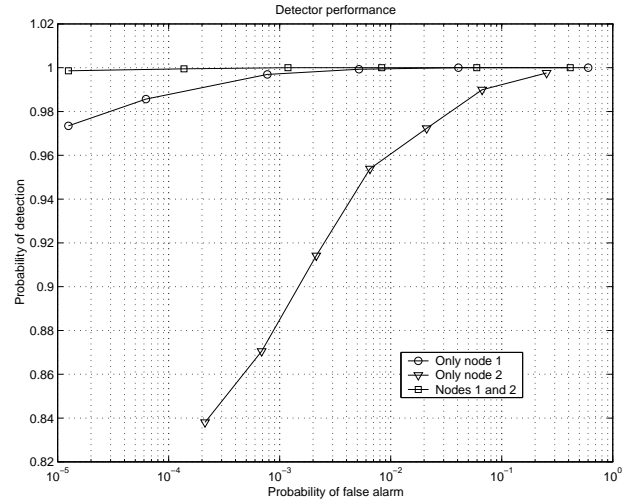


Fig. 4. The performance of the detector

of false alarm, 80000 blocks of RSSI values were recorded with closed door. To calculate the average probability of detection, 16000 blocks of RSSI values were recorded with half-open door. The detection procedure was carried out using data from only the first receiver node (Node 1), from only the second receiver node (Node 2) and from both nodes (Nodes 1 and 2) with the proposed algorithm. The resulting detector performance curves can be observed in Figure 4. As can be seen, by increasing the number of nodes, the detection performance can be significantly improved. In case of single-node detection, it is possible to achieve a certain performance, but combining the information coming from different nodes with the appropriate fusion function will result in higher probability of detection at any given probability of false alarm.

## 6. CONCLUSIONS

We considered the problem of using multi-node wireless networks for distributed surveillance, adding another functionality to the standard communication functionality of such networks. The surveillance functionality is implemented by using a wireless communication network as a wireless sensor network. We developed a multi-sensor model for the received signal parameters of interest, and devised distributed estimation, information fusion and detection algorithms to implement the surveillance functionality.

## 7. REFERENCES

- [1] A. Kara, H. L. Bertoni, "Blockage/Shadowing Polarization Measurements at 2.4GHz for Interference Evaluation between Bluetooth and IEEE 802.11 WLAN", *IEEE Antennas and Propagation Society International Symposium*, Vol. 3, pp. 376–379, 2001.
- [2] K. Pahlavan, *Wireless Information Networks*, Wiley & Sons, 1995.
- [3] J. Sørensen, Z. Safar, J. Chen, K. Kristoffersen and M. Schiøtz, "Indoor Surveillance with Multimodal Wireless Networks", submitted to *IEEE ISSPIT*, June 2004.